HiSST: 3rd International Conference on
High-Speed Vehicle Science Technology
14 -19 April 2024, Busan, Korea

# Frequency Modulation Analysis in Innovate Supersonic Cavity Flow

*Ting Tsung Chang[1], Konstantinos Kontis[2]*

## Abstract

Modulation characteristics of the cavity still inspire people to study through a variety of mathematic approaches. The primary purpose here is to apply not only conventional fast Fourier transform but continuous wavelet transforms to study the spectrum of different cavity flow configurations experimentally. Via modulation analysis, we find that the suggested modulation parameter, normally 0.25, in the theoretical model is not always constant. Since the shear layer impingement on the trailing-edge is the dominant source driving the aeroacoustic mechanism, the angled ramp significantly alters its development, and the level of the pressure tone drops dramatically. An innovative passive control method with sub-cavity introduced recently is studied in this paper as well. The sub-cavity applied on the aft wall, however, considerably amplifies pressure tones inside the sub-cavity and induces extra modes by fluidic resonance. Moreover, the frequency spectrum of AM of individual Rossiter mode indicates the interaction between each mode.

**Keywords: Supersonic Cavity Flow, Frequency Modulation, Sub-Cavity**

## Nomenclature

D – Cavity depth
dB – decibel
f – frequency
L – Cavity length
l – sub-cavity depth
M – Mach number
n – number of Rossiter mode
Re – Reynolds number per ft
r – cavity recovery factor
k – the ratio of the convective velocity of vortices to the free stream velocity
U – flow velocity
W – Cavity width

Greek
$\alpha$ – modulation constant
$\gamma$ – specific heat ratio

Others
$\infty$ – free stream

## 1. Introduction

Cavity flow has drawn much attention for years due to its critical role in aviation applications, from internal weapon bay to supersonic combustion ramjet, or known as scramjet, where the cavity is employed as a flame holder. Flow, either subsonic or supersonic, over the cavity inevitably generates a high-pressure tone considering aeroacoustic resonance. This is particularly undesirable from a structural standpoint. Moreover, the adverse pressure distribution inside the cavity might pose a potential danger to weapon release during high-speed flight [1-2]. Speaking of the application of flame holders, engineers hope to take advantage of the flow circulation inside the cavity to increase the combustion efficiency [3].

Earlier research started from well-known Krishnamurty [4], Roshko [5], and Rossiter [6], who pioneered this topic with their physical model to predict pressure oscillation inside a cavity and to establish the understanding of flow physics experimentally or numerically. They concluded that the periodic oscillation is essentially induced by the shedding vortex from the front lip of the cavity and by radiation from the trailing edge. Among them, Rossiter proposed a model that is generally regarded as a milestone in building a physical model with certain accuracy compared to experimental data, and the oscillation frequencies existing in cavity flow are named Rossiter modes thereafter. Later, a modified

model introduced by Heller [7] significantly improved the accuracy of the prediction of pressure oscillation tone and this model has been more widely adopted ever since:

$$\frac{fL}{U_\infty} = \frac{n-\alpha}{M_\infty[1+(^{r}/_{2})(\gamma-1)M_\infty^2]^{-0.5}+(^{1}/_{k})} \quad (1)$$

Numerous studies have been carried out to alleviate the high-amplitude and high-frequency pressure oscillation and, at the same time, to understand the physical mechanism behind it. To achieve this, some innovative schemes are introduced to study their corresponding effects. Ranging from leading-edge modification, for instance, spoilers, rods, or sawtooth-edge to trailing-edge ramps, these passive schemes show their effectiveness in different Mach numbers [8,9]. They all aim to alter the development of the leading-edge shear layer development which causes the instability inside the cavity so that the resonant mechanism is weakened. Vikramaditya [10] systematically conducted experiments on cavities with various aft wall ramp configurations. From his shadowgraph results, he noted that the wavy shear layer over the cavity with a ramp angle of 90 to 45 degrees seemed to be weakened. The decreasing OSPL distribution then evidentially proved that the cavity flow is stabilized. More recently, sub-cavity has showcased its ability in pressure suppression and has become highlighted by many researchers [11]. It is inspiring that sub-cavity could be served as either a suppressor or resonator.

In Rossiter's model, the aeroacoustic is established on the periodic vortex-shedding. Therefore, in general, the traditional Fast Fourier transform (FFT) can detect those principal modes from pressure recording with great agreement. Nevertheless, the oscillation inside the cavity is neither non-periodic nor nonstationary. To be more comprehensive in such a complicated flow structure advanced mathematical approaches are required so that the temporal behaviour can be properly studied. Several have applied different approaches, short-time Fourier transform (STFT) for instance, to investigate the so-called mode switching in cavity flow [12]. Not being observed by FFT, STFT reveals that modes are not presented continuously in time but rather in an intermittent manner. Nevertheless, STFT has poorer temporal-frequency resolution. Hence, studies with better temporal resolution are carried out through continuous wavelet transform [13]. It shows that even the most dominant mode in the spectrum is rather sporadic.

The primary aim of this article is to investigate the modulation feature of the cavity with sub-cavity implemented on trailing-edge as well as aft wall ramp configurations. Comparisons are made to examine the overall influence of different geometry changes in the SPL. Additionally, spectral analysis is carried out to discourse the oscillatory feature of pressure tones in various configurations respectively. To achieve this, not only conventional FFT is used to figure out the Rossiter modes but continuous wavelet transform is applied to study the temporal distribution of a specific mode and its amplitude modulation.

## 2. Experimental Details

### 2.1. Wind Tunnel Facility and Experimental Setup

The supersonic wind tunnel experiments were conducted in an indraft-type facility located at the Argyll wind tunnel complex of the University of Glasgow. The models are implemented in the test section whose cross-section is 101.6 mm x 54 mm, as illustrated in Fig.1. The wind tunnel is connected to a large tank whose volume is approximately 35 $m^3$ and is vacuumed to sustain steady operation at Mach 1.6 for 10 seconds maximum. The Reynold's number, Re, based on average room temperature, 293 °k, and stagnation pressure, 101 kPa, measured in the settling chamber is around $4.6X10^6$ per feet. Statistic pressure, as our reference pressure, is measured by RS Type 797-4970 pressure transducer flush mounted on the side wall at the beginning of the test section. Dynamic pressure signal, on the other hand, is obtained by multiple Kulite sensors flush mounted on the cavity floor, front wall, and aft wall. The layout is schematically shown in Fig.2. These Kulites are wired to our data acquire system comprising National Instrument cDAQ series hardware and homebuilt code by LabView. The data is sampled at 100K Hz for 2 sec. and is pre-filtered by a 30k Hz digital low-pass filter. The raw data is then divided into 96 segments with a 50 % overlap of 4096 samples. This gives us a resolution of 24.4 Hz. Since a variety of models are applied in our study, code names are given, listed in the following Table.1, respectively so as that data can be systematically sorted and the reader can easily compare the difference of their outcomes. Our investigation mainly focuses on open-type cavities with L/D = 4 and W/D = 8.4, and its dimensions are sketched in Fig.2.

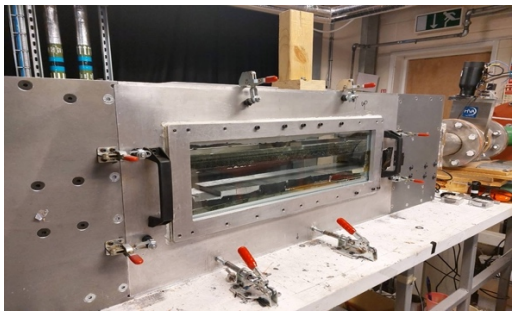

**Fig. 1** Our Supersonic wind tunnel in the Argyll facility

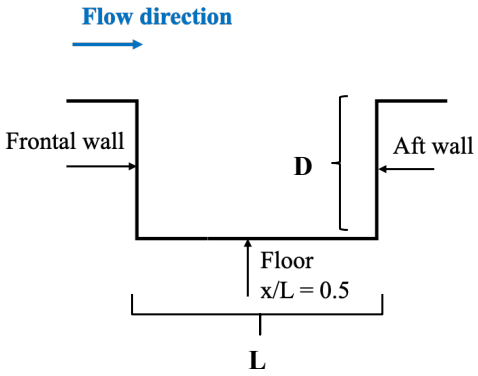


**Fig. 2** The general layout of locations of sensors and the dimension of the cavity

**Table 1.** Code names of test configurations in our study

| Code Name | L/D | Remark |
|---|---|---|
| B4 | 4 | Baseline |
| BR45 | 4 | Trailing-edge 45-degree ramp |
| BTS4 | 4 | Trailing-edge sub-cavity (l/L = 0.25) |

### 2.2. Power Spectral Density

The power spectral densities of unsteady pressure were computed by self-build MATLAB code. The pressure data is processed by fast Fourier transform (FFT) to obtain its frequency spectrum and it is converted into sound pressure level (SPL) thereafter by the following definition:

$$SPL(f) = 10\log_{10}\frac{PSD(f)}{p_{ref}^2} \tag{3}$$

where PSD stands for power spectral density and $p_{ref}$ is the reference pressure set to be $2\text{x}10^{-5}$Pa

### 2.3. Continuous Wavelet Transform

The wavelet transform approach is a practical tool to analyze the signal in the time-frequency domain. By adopting wavelet, it is possible to project a signal onto a range of scaled and translated mother wavelet yielding better frequency resolution. The definition of continuous wavelet transform is defined as

$$W(a,\tau) = a^{-1/2}\int_{-\infty}^{\infty} f(t)\psi^*(\frac{t-\tau}{a}) \tag{4}$$

where $\psi$ is the wavelet function or the mother wavelet, and $a^{-1/2}$ is the normalization factor. In our study, the Morlet wavelet is applied considering its mathematical characteristics. The complex expression enables the Morlet wavelet properly to capture oscillation since both amplitude and phase

can be acquired. Some reference has clearly shown the capability of Morlet wavelet in turbulence analysis [13]. Morlet wavelet is mathematically defined as:

$$\psi(t) = \exp(\mathrm{i}\omega_\psi \mathrm{t})\exp(-|t^2|/2)$$

where $\omega_\psi \in [5,6]$ is a constant that forces the admissibility.

## 3. Result and Discussion

### 3.1. Unsteady Pressure Analysis

The frequency spectrum of the unsteady pressure with various configurations is clearly shown in Fig.3. Rossiter modes are vividly observed, with the first three modes being dominant in the spectrum, while the 1st mode is insignificant. In Woo's study [14], he indicated that the 1st mode is highly incorporated with flow structure in the spanwise direction. As he concluded, a high W/D ratio inevitably caused the reduction in the 1st mode and characterized with strong the 2nd mode. For the remaining modes, their values are moderately deviated from the theoretical prediction in the baseline case. Nevertheless, according to Tam [15], the perfect match on the theoretical values does not essentially guarantee the correct modeling since the theoretical values according to Eq. 1 are obtained with generally used constants, r = 0.89, k = 0.57, and $\alpha$ = 0.25. Hence, it is not surprising that there is a certain departure based on experimental data since these empirical constants always change according to different Mach numbers or the upstream boundary layer condition. For instance, the constant, k, has its suggested values ranging from 0.5 up to 0.75. To further investigate the physical mechanism and to find out the proper value for the model, we carry out frequency modulation analysis, proposed by Delpart [16], for a more accurate value. The averaged fundamental frequency, $f_a$, is 3255 Hz compared to 3437 Hz theoretically evaluated by Eq. 3. Noted as modulation frequency, $f_b$, the experimental value is 850 Hz while the theoretical value evaluated by Eq. 4 is 859 Hz. Consequently, the modulation parameter, $\alpha$, is 0.26 rather than 0.25 which is universally used.

$$f_a = \frac{U_\infty}{D}\frac{1}{M_\infty[1+(^r/_2)(\gamma-1)M_\infty^2]^{-0.5}+(^1/_k)} \tag{5}$$

$$f_b = \frac{U_\infty}{D}\frac{0.062}{M_\infty[1+(^r/_2)(\gamma-1)M_\infty^2]^{-0.5}+(^1/_k)} \tag{6}$$

The slight difference in this parameter again shows this frequency modulation will change with different conditions. Right next to the second primary mode, there is a minor peak, at around 6300 Hz. According to Kegerise's study [12], it might be induced by the non-linear interaction between each Rossiter mode. However, without higher-order analysis, we are not able to make a concrete conclusion, and it is beyond the scope of the presenting study. The application of a ramp substantially suppresses the pressure oscillation in two perspectives. First, as presented in the Fig.3(b), the second mode and third mode are dramatically annihilated. Second, in general, the broadband spectral level slightly decreases. As pointed out by [10], the ramp can fundamentally stabilize the shear layer development and the fluctuation radiated from shear layer impingement is interrupted.

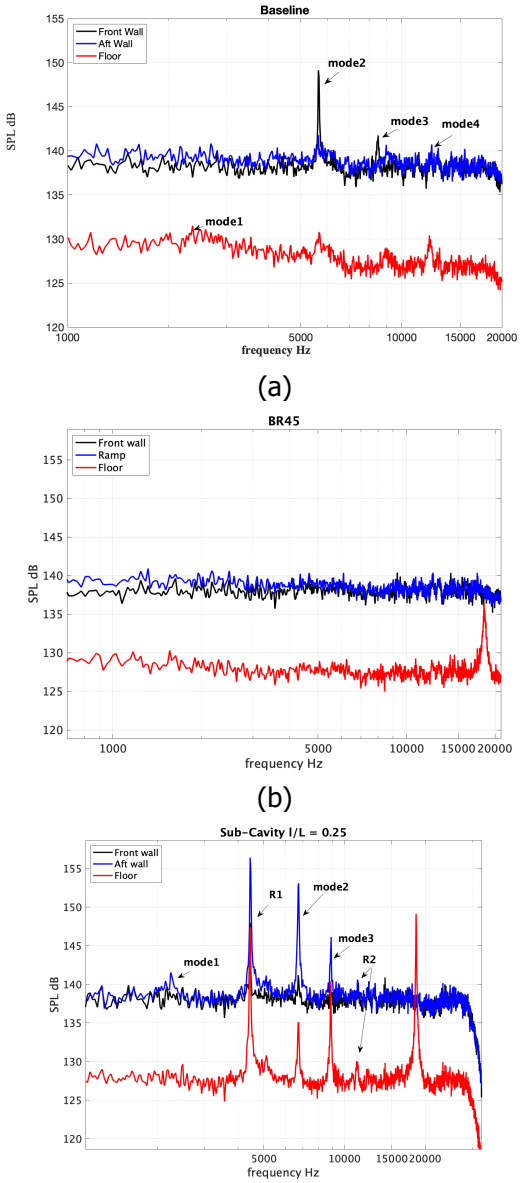


**Fig. 3** Frequency spectrum of unsteady pressure signal (a) Baseline (b) 45-deg ramp (c) Sub-cavity

The sub-cavity whose depth ratio, l/L, is 0.25, essentially presents an entirely different result as shown in Fig.3 (c). Still, the Rossiter modes are visible over the spectrum while new non-Rossiter modes are captured. Rossiter modes on the frontal wall, compared to the baseline case, are largely suppressed. For instance, the 2$^{nd}$ mode has approximately 141 dB, while in the baseline case, this value is as high as 149 dB. Nonetheless, the spectrum inside the sub-cavity presents an opposite phenomenon. Those modes are considerably gained by at least 6 dB. Those newly induced frequency peaks, noted by *R* in the plot, however, characterize themselves with unique frequencies. According to Kevikumar's study [11], he noted that such frequency is not associated with fluid dynamic etc. Rossiter mode, but fluid resonance. The flow is entrained into the sub-cavity as if the flow traveled inside a closed duct resulting standing wave. These two resonant modes, R1 and R2, are located at 4443 Hz and 11084 Hz respectively. In addition, Kevikumar stated that the depth ratio of the sub-cavity plays a critical role in the frequency spectrum. Fluidic dynamic modes and fluidic resonance modes might coexist simultaneously with certain l/L while the Rossiter modes will be annihilated with higher values. In our study, we perfectly demonstrate the coexistence of both.

To verify our assumption of flow stabilization due to different geometries, quantitative identification is made through the probability density function (PDF) of the pressure fluctuation data. Rowley [17] pointed out that, derived from dynamic stability theory, the PDF of random data can represent the

stability of the dynamic system. Later, Smith [18] also demonstrated that the shrinking PDF of the pressure fluctuation implies the stabilization process. For a given Mach number, a broader distribution is caused by large variance due to high intermittentness, etc. high turbulence intensity. Therefore, as shown in Fig.4, the probability density function of the pressure data gradually narrows toward central with the implementation of either ramp or sub-cavity giving the hint that pressure fluctuation caused by the fluidic dynamic instability is effectively suppressed. The Gaussian-like distribution indicates that the flow structure is mainly featured with broadband, stochastic noise [16]. Therefore, it is reasonable to calculate the associated statistical index and make a comparison with the standard normal distribution. On the front wall, all three cases have moderate departure from normal distribution, while it is the sub-cavity that has the closest value of kurtosis, 3.03, compared to 3 in standard normal distribution, on the cavity's floor. On the other hand, in terms of skewness, it is the BR45 that has the closest value to the normal distribution.

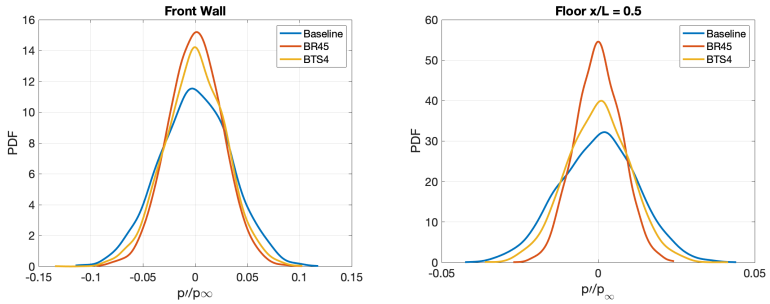


(a) (b)

**Fig.4** Probability density function of pressure oscillation (a) front wall (b) x/L = 0.5

### 3.2. Continuous Wavelet Spectrum Analysis

The normalized scalogram obtained from CWT presents intermittent behavior of actual aeroacoustic phenomenon in supersonic cavity flow. The sporadic pattern of individual modes evidentially shows that they are non-stationary and aperiodic. The second mode as well as the third mode occupy the most of the energy in all spectrums as seen in Fig.5 whereas, with a closer look, the 1st mode, which is hardly observed in the Fourier spectrum, is captured but in a relatively weak manner. In ramp configuration, the CWT results indicate that Rossiter modes still exist. They are relatively weak compared to the baseline case since the ramp significantly suppresses the pressure oscillation and its feedback mechanism.

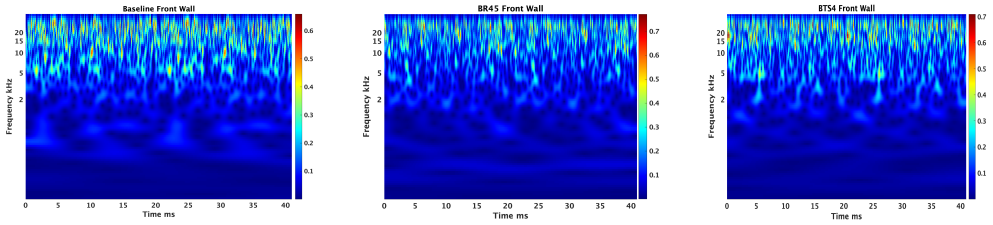


(a) (b) (c)

**Fig.5** Front wall CWT scalogram of all configurations (a) B4 (b) BR45 (c) BTS4.

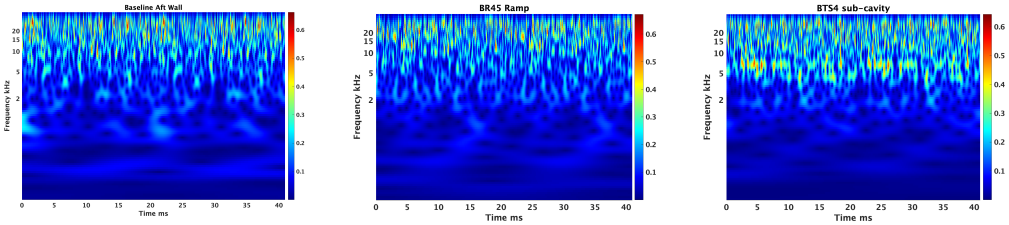


(a) (b) (c)

**Fig.6** Rear wall CWT scalogram of all configurations(a) B4 (b) BR45 (c) note that this result is obtained inside the sub-cavity, BTS4.

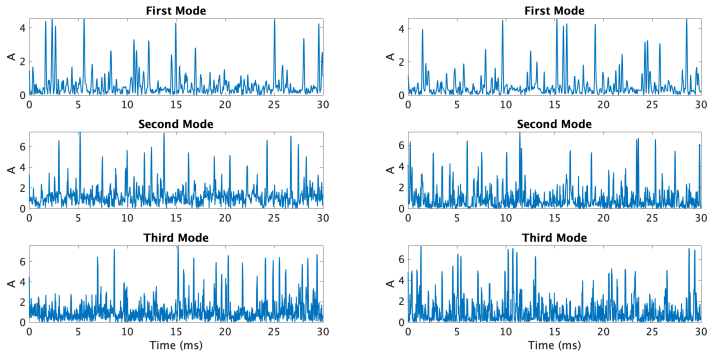


(a) (b)

**Fig.7** Front wall amplitude modulation at three Rossiter modes (a) B4 (b) BTS4

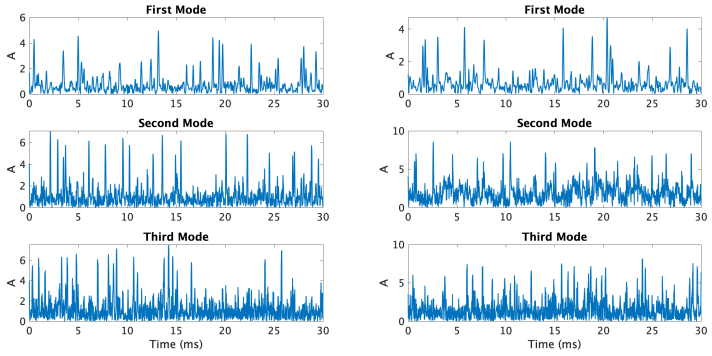


(a) (b)

**Fig.8** Rear wall amplitude modulation at three Rossiter modes (a) B4 (b) note that the result is obtained inside the sub-cavity, BTS4

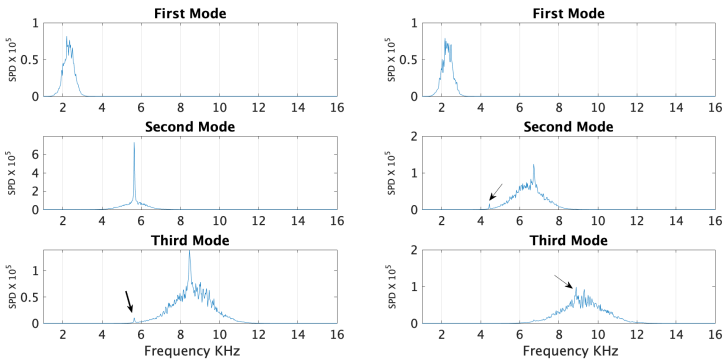


(a) (b)

**Fig.9** SPD of amplitude modulation on the frontal wall (a) B4 (b) BTS4

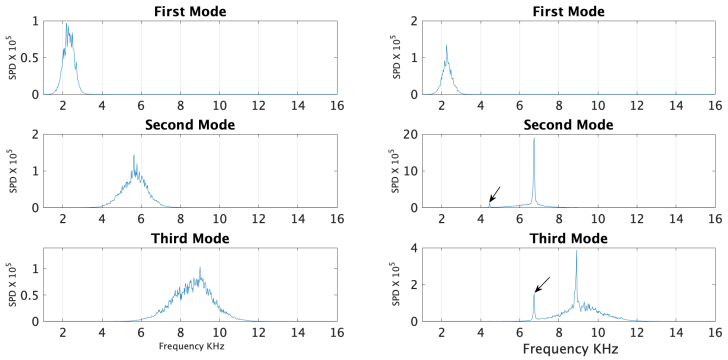


**Fig.10** SPD of amplitude modulation on aft wall (a) B4 (b) BTS4

Scalograms of BTS4 clearly illustrate the distinctive pattern. As mentioned previously, Rossiter modes are essentially amplified inside the sub-cavity. The 2nd mode in particular shows very energetic behaviour over time and it occurs more frequently than that in the baseline case. Moreover, those resonant modes are vividly observed in the scalogram. Taking the second resonant mode which is noted as R2 in the Fourier spectrum, for example, in Fig.6 (c), it occasionally shows strong intermittency in the spectrum.

The major advantage of the wavelet is that it can serve as a band-pass filter extracting specific frequency components. In both Fig.7 and Fig.8, we pick up the normalized energy at the first three modes respectively. The result indicates that the amplitude modulation (AM) is changing with time. Amplitude modulation on the front wall has approximately the same level in both the 2nd and 3rd modes, while the 1st mode is slightly less energetic. It is also worth noticing that the level of AM remains quite the same on frontal and aft walls. This result is different from other studies. We suspect that this is due to the high W/D ratio of the cavity but we need to obtain evidence to prove it. On the other hand, on the aft wall, the AM of the 1st mode is relatively weak, and that in the 3rd mode is relatively stronger. In terms of BTS4, the AM in 1st mode on the frontal wall is less powerful than the other two modes. In comparison, sub-cavity has stronger AM than the baseline, on the aft wall. In addition to the scale of AM in the time domain, it is worthwhile to study its spectrum. As we have extracted certain frequency components, it is expected that its spectrum will present a clear and predominant peak at the corresponding frequency. As indicated in Fig.9 and Fig.10, the frequency peak is captured at the corresponding mode. At the third mode on the frontal wall, in Fig.9, the frequency associated with the second mode, highlighted by an arrow, is also observed while this does not take place on the aft wall. The results from sub-cavity essentially disclose a more unique structure. The 2nd mode is not only modulated by its principal frequency, but the resonant frequency pointed out by an arrow. Moreover, the 3rd mode on the front wall is characterized by another frequency at around 8000 Hz, and that on the aft wall is modulated by the 2nd mode simultaneously. The cause of the split of the peak in the spectrum, however, remains unknown here. More studies are indeed required in the future.

## Conclusion

The primary object of this study is to apply both FFT and CWT to disclose the modal characteristics in different geometries. First, the modulation coefficient generally used in theoretical prediction is not constant in all circumstances. It changes according to various conditions, and geometry. The trailing-edge ramp has proved to be a powerful approach to stabilize the vortex induced by fluidic dynamic instability through our PDF results and, consequently, dramatically reduces the sound pressure level of certain modes. In terms of sub-cavity, there are two findings. First, the SPL of Rossiter modes inside the sub-cavity is greatly enhanced considering the standing wave-like feedback. Though the result is completely in contrast to our original goal, it provides another option for application in cavity flow. Second, the induced fluidic resonant frequencies in light of standing wave-like feedback are observed. Continuous wavelet transform provides more insightful information in the temporal-frequency domain due to its mathematical characteristics. The spotty behaviour of all modes including typical Rossiter modes as well as the fluid resonant mode observed in the sub-cavity case are vividly captured. The frequency spectrum of amplitude modulation shows that some certain mode is not purely caused by a

single frequency but by multiples. There is an interaction between neighbouring modes. Further research is required to be done systematically in the future i to fully explore the physical mechanism of sub-cavity and the effect of a high W/D ratio of the cavity on aeroacoustic oscillation.

## Reference


1. Rodney, L. Clark.: Evaluation of F-111 Weapon Bay Aero-acoustic and weapon separation improvement techniques. AFFDL-TR-79-3003. (1979)
2. Essam, F. Sheta, Robert E. Harris, Benjamin George, Lawrence Ukeiley, Edward Luke.: Loads and acoustics prediction on deployed weapons bay doors. Journal of Vibrations and Acoustics. (2017). https://doi.org/10.1115/1.4035701
3. Dora Musielak.: Scramjet Propulsion: A Practical Introduction. (2023)
4. Krishnamurthy, K.: Acoustic radiation from two-dimensional Rectangular cutouts in aerodynamic surfaces. NASA-TN-3487. (1955)
5. Roshko, A.: Some measurement of flow in a rectangular cutout. NACA-TN-3488. (1955)
6. Rossiter J.: Wind tunnel experiment on the flow over rectangular cavities at subsonic and transonic speeds. NACA-TR-3488. (1964)
7. Heller, H. H., Holmes, D. G., Covert, E. E.: Flow-induced pressure oscillation in shallow cavities. Journal of Sounds and Vibrations. Vol. 18, No.4, pp. 545-553. (1971)
8. Saddington, A. J., Thangamani, V., Knowles, k.: A comparison of passive control methods for a cavity in transonic flow. Journal of Aircraft. (2016) http://dx.doi.org/10.2514/1.C033365
9. Wang Xiansheng, Yang Dangguo.: Control of pressure Oscillations induced by supersonic cavity flow. AIAA Journal. Vol. 58, No. 5. (2020)
10. Vikramaditya, N. S., Kurian, Job.: Pressure oscillation from cavities with ramp. AIAA Journal. Vol. 47, No. 12. (2009)
11. Lad, Kevikumar A., Vinil Kumar, R. R., Vaidyanathan, Aravind.: Experimental study of subcavity in supersonic cavity flow. AIAA Journal. Vol. 56, No. 5. (2018)
12. Kegerise, Michael A., Spaina, Eric F., Garg Sanjay, Cattafesta, Louis N.: Mode-switching and nonlinear effects in compressible flow over a cavity. Physic of Fluid. (2004) http://dx.doi.org/10.1063/1.1643736
13. Jordan, D., Miksad, R. W., Powers, E. J.: Implementation of continuous wavelet transform for digital time series analysis. American Institute of Physics. (1997)
14. Woo, Chel-hun, Kim, Jae-soo, Lee, Kyung-hawn.: Three-dimensional effect of supersonic cavity flow due to the variation of cavity aspect and width ratios. Journal of Mechanical Science and Technology. (2008) https://doi.org/10.1007/s12206-007-1103-9
15. Tam, Christopher K. W., Block, Patricia J. W.:On the tones and pressure oscillations induced by flow over rectangular cavities. J. Fluid Mech. Vol. 89, part 2, pp373-399. (1978)
16. Delprat, N.: Low-frequency components and modulation process in compressible cavity flows. Journal of Sound and Vibration. https://doi.org/10.1016/j.jsv.2010.05.013
17. Rowley, Clarence W., Williams, David R., Colonius Tim, Murray Richard, Macmynowski, Douglas G.: Linear models for control of cavity flow oscillations. J. Fluid Mech. (2006) http://doi.org/ 10.1017/S0022112005007299
18. Smith Eric, Kumar Rajan.: Dynamic pressure measurement in a rectangular cavity with multiple stores. AIAA Journal. (2023) https://doi.org/10.2514/1.J062934